

# DESIGNING AN UNDERWATER EEL-LIKE ROBOT AND DEVELOPING ANGUILLIFORM LOCOMOTION CONTROL

NSF Summer Undergraduate Fellowship in Sensor Technologies

Tamara Knutsen, Harvard University

Advisors: Professor Jim Ostrowski (GRASP Lab), and Kenneth McIsaac (GRASP Lab)

## ABSTRACT

In this report, I investigate the design and development of an eel-like amphibious robot. After reviewing research on dynamic mobile robots and control and motion planning for biomimetic robot systems, I analyzed the prototype created by Kenneth McIsaac and Jim Ostrowski and redesigned its key mechanical, electrical and communication components. The significant changes I implemented affected the number of links of the robot, its waterproof characteristics and the communication design (both hardware and software). I designed and manufactured the mechanical components using the state-of-the-art CAD/CAM facilities at the University of Pennsylvania and assembled and waterproofed the prototype at the GRASP laboratory. McIsaac and I made the necessary modifications to the open-loop control of the robot and at the time of writing this report, the prototype seems to be functioning as expected. The closed loop control of the robot is still being developed at this time.

## 1. MOTIVATION

Robotic research is driven by the challenge of extending robot technology to all environments, especially those inaccessible to humans. My interest lies in anguilliform locomotion control of an amphibious mobile robot that can traverse uneven terrain or confined spaces like tunnels or pipes using serpentine motions and three-dimensional dynamic aquatic environments using eel-like motions. This technology can be directly applied to the exploration, monitoring and surveillance of highly constrained and inaccessible environments such as nuclear reactor cores, underground toxic waste tanks, and deep-sea exploration as well as to the human intestine and circulatory system (on a microscopic scale).

The foundations for this research are developed from recent work in many converging fields of interest. A brief review of current research in these five fields: underwater robotic systems; biomimetic robotic technology; biological models of locomotion; a unified geometric model of underactuated mobile mechanical systems; control algorithms for dynamic robot locomotion, will further illuminate the motivations for this research endeavor and help characterize the problems inherent in this project. The main considerations for this mobile robot project are to increase the robot's agility, maneuverability and efficiency, to expand the range of environments accessible to the robot and to develop robot motion planning and control.

## 1.1 Underwater Robotic Systems

Previous underwater robotic systems have emphasized larger vehicles like Woods Hole's JASON (see Fig. 1) [3,4]. The research for such robot systems has focused on developing the communication in real-time technologies, without much concern for agility, efficiency or maneuverability of the system. With increased efficiency (better methods of locomotion), an underwater robot would require less energy to accomplish the same task. Lower energy requirements would feasibly allow batteries as the energy supply (allowing the mobile robot to be untethered). Increased agility and maneuverability are linked to a general decrease in the size of the robot as well as more flexibility in the internal shape of the robot. In order to improve these properties of the robot systems, researchers have begun studying aquatic biological systems and their methods of locomotion.

## 1.2 Biomimetic Robotic Technology

Biomimetic robots mimic biological systems or utilize technology developed from designs found in nature. Recent research efforts have developed a range of carangiform (fish-like) robots. MIT's RoboTuna and RoboPike projects are attempts to create autonomous underwater vehicles (AUVs) with increased energy savings and running-life time, by using a flapping

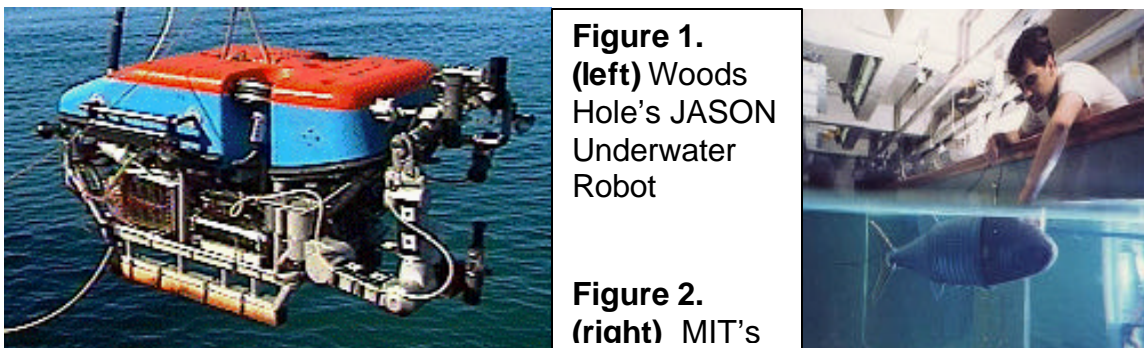


**Figure 1.**  
**(left)** Woods  
Hole's JASON  
Underwater  
Robot

**Figure 2.**  
**(right)** MIT's

foil (tail fin) that exploits external fluid forces to produce higher accelerations and lower energy consumption compared to a typical propeller of a submarine-type vehicle like JASON (see Fig. 2) [5, 6]. Legged biomimetic underwater robots able to crawl omnidirectionally on the ocean bottom as well as on land, can traverse a broad range of environments, but are not able to navigate the water column above the ocean bottom (see Fig. 3, 4) [7, 8, 9].

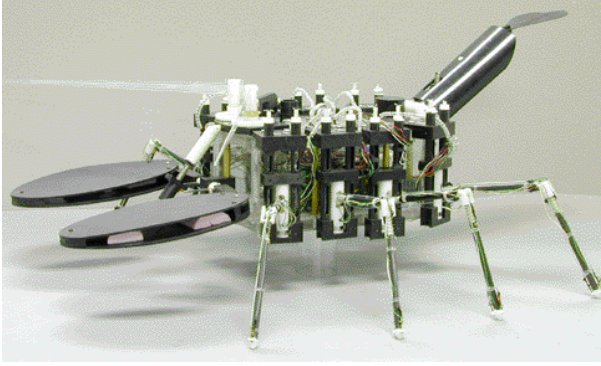


**Figure 3.** Northeastern University's Ambulatory Underwater Robot



**Figure 4.** ISRobotics Ariel Robot

Research into robotic technology that can move dynamically in three-dimensions led to the development of hyper-redundant manipulators, redundant manipulators where the relative degree of redundancy is either a very large number (from the number of relatively identical rigid links) or infinite (the case of a relatively homogeneous flexible physical structure) [1]. Hyper-redundant manipulators are classified into two groups. Tensors (manipulators with a fixed body length) mimic the morphology and function of snakes, elephant trunks or tentacles. Extensors (manipulators with elastic bodies or elastic sections between rigid links that can be stretched and contracted to change the overall body length) mimic more elastic animal bodies like invertebrates, such as slugs and worms. Robotic manipulators with high or infinite number of degrees of freedom can operate in highly constrained environments and articulate a larger range of motions than other systems because they have greater adaptability and versatility in their shapes.

In the case of navigating a water column, Northeastern University has developed an undulatory underwater robot using shape-memory alloys and a number of links (see Fig. 5) [7]. This lamprey-like robot is able to move through the water column, using lateral undulations to propel itself forward similar to the robot fish, and to change its depth. However, it is not capable of transitioning to land locomotion. My project is to develop an undulatory mobile robot that can navigate the aquatic (ocean bottom and water column) and terrestrial environment. Another goal of this project is to develop closed-loop control of the eel, which requires an understanding of the different gaits necessary to navigate to a desired destination. An eel-like model was developed from a combined biological model of the American Freshwater Eel, *Anguilla rostrata*, since these eels were shown to have short terrestrial excursions, and the Swimming Eel, *Anguilla vulgaris*, the first eels studied in order to characterize their swimming kinematics (see Fig. 6) [10, 11]



**Figure 5. (above)** Northeastern University’s Undulatory Underwater Robot  
**Figure 6. (below)** *Anguilla rostrata*, the American Freshwater Eel.



### 1.3 Biological Models of Locomotion

The swimming behavior of flexible elongate fish was first described as the “anguilliform mode” by Breder, who categorized these fish under the genus name *Anguilla* [10]. In a pioneering study of the kinematics of fish and eels, Gray tried to relate patterns of axial movements during swimming to the production of forward thrust, from photographic frames of a juvenile *Anguilla vulgaris* [11]. He noted that waves are produced anteriorly and passed posteriorly with increasing amplitude in order to create propulsive force. Aquatic locomotion is possible because water resists motions perpendicular to the direction of travel more than parallel motions due to the shape of the organism, so eels push their curves against the resistance of the water. Gillis studied adult *Anguilla rostrata* swimming kinematics and noticed that the anterior 20% of these eel bodies do not undulate during swimming [12]. The reason for the difference between Gray’s and Gillis’ studies is due to the size and not to the species. Gillis noted that smaller fish use movements with higher relative amplitudes than larger fish. Smaller fish accelerate by increasing tail-beat frequency and tail-tip amplitude (stride length and mechanical efficiency tend to increase as speed increases). Larger fish increase speed by increasing percentage of body that is undulating and increasing tail-beat frequency (but tail-tip amplitude, stride length and mechanical efficiency are constant, as the speed increases). For the work presented here, however, a simplified kinematic model that is a generalization for all eel species is used.

Similarly, Hirose and others have characterized land-based snake locomotion into four distinct gaits, cyclic patterns of input that yield non-zero motion over one cycle [13]. These four gaits are: serpentine motion (undulating motion that a snake uses to propel itself forward by leveraging the hind part of each curve against irregularities in the ground);

rectilinear motion (used by large, heavy snakes to slowly glide whole body forward in a straight line); concertina motion (spring-like motion used by snake to pull itself forward or to climb) and sidewinding (sideways stepping used by snakes in environments with little lateral friction like shifting sand) (see Fig. 7 for further explanation). For land-based

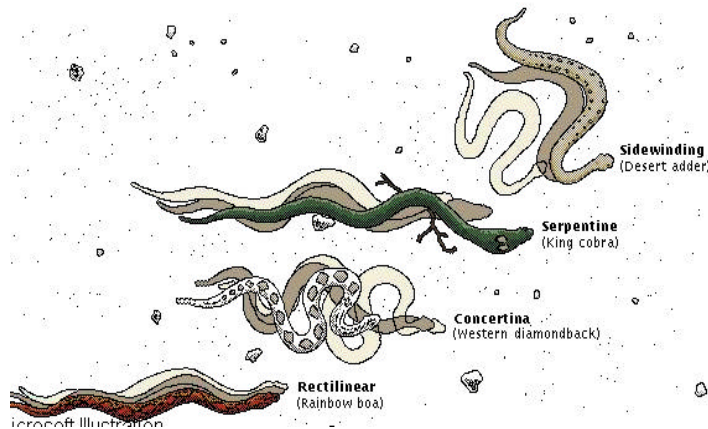


**Figure 8.** Characterization of a snake cross-section (left) and an eel cross-section (right). Note lateral

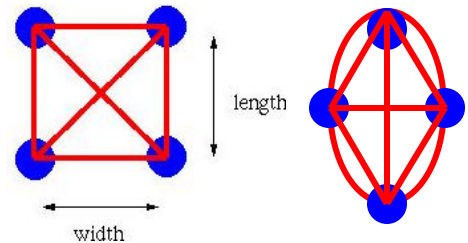


**Figure 7. (above)**

**Rectilinear motion** is forward gliding by pushing groups of belly scales against the ground while sliding others forward.

**Concertina motion** is a caterpillar-like forward motion by bunching and lengthening its strong muscles in a spring-like manner.

**Serpentine motion** [1] is a muscular creeping of the body using both: a sinusoidal waveform that moves along the curvature of the body (formulated as the serpenoid curve) and a sinus -lifting that functions to prevent slippage (the action by which one part of the body floats up during advancement to concentrate the body weight on the part that can most easily slip).

**Sidewinding** [3] is sideways stepping by first throwing out a lateral arc with its head and the front part of its body, then transferring the rest of its bulk to this forward purchase, then repeating the first step. [14]

locomotion to occur, lateral resistance must be greater than ventral friction. A snake's body has been characterized as a series of linked squares, which emphasizes the importance of the bilateral ventral friction when compared to the elliptical cross-section of an eel (see Fig. 8). Gillis found that locomotion of American eels on land, though very different from locomotion in water, was only slightly different from each of the land-based snake gaits, and may in fact be a composite of these gaits (to maximize forward motion despite low lateral resistance and high ventral friction) [12]. For simplicity, we will use a generalized serpentine model of land-based biological motion.

#### 1.4 Mathematical Models of Locomotion

Grillner and Kashin elucidated the neural network underlying undulatory axial muscle motions by studying the much simpler nervous system of lampreys, an ancient, simple, elongated fish. They noticed that the body undulations are caused by motoneuronal activity that oscillates on either side of the spinal cord as it travels caudally (see Fig. 9) [15]. Control of movement is maintained by lateral excitatory, lateral



inhibitory, contralateral inhibitory and edge cell neurons that alternately activate the motor neurons down the length of the spinal cord.



**Figure 9.** Side view of a lamprey (left) and top view of parasitic lamprey attached to host fish (right).

Ekeberg incorporated these studies into his computer simulation of lamprey swimming, developing both the neural network model and mechanical model to directly agree with the dimensions and specifications in the lamprey studies [15]. Ekeberg successfully simulated the entire locomotion system, coupling the effects of the shape changes in the lamprey controlled by the neural network to the external drag forces of the water. Utilizing Ekeberg's discrete mechanical model, characterization of approximate external and internal forces and a simplified model of control (instead of considering the actual structure of the neural network) simplifies the model to the essential inputs to be sent to each mechanical link in order to control the overall motion. McIsaac and Ostrowski were able to geometrically analyze different gait patterns on the anguilliform motion model [16].

By framing robotic locomotion systems (underactuated robots that move through their environments) into a geometric description, we can determine the entire behavior of the dynamic system from a simple set of inputs. These inputs may or may not directly actuate the system dynamics. An underactuated mechanical system is a system in which some or most of the dynamics are actuated indirectly (control inputs to other parts of the system result in motion in another part of system or in motion of the entire system).

For mobile robots, the inputs usually specify the internal shape of the system. The dynamics of a mobile robot system are derived from the coupling of these inputs to constraints or external forces on the system when considered in a context that includes its environment. By decoupling a dynamic complex system into these elements, we can similarly decompose and simplify the motion-planning problem for such a system and then structure it into control algorithms for the robot. The mathematical models for these decompositions and abstractions are presented below in the section on anguilliform locomotion and are supported and described in detail in the other papers listed in the references [see section 5].

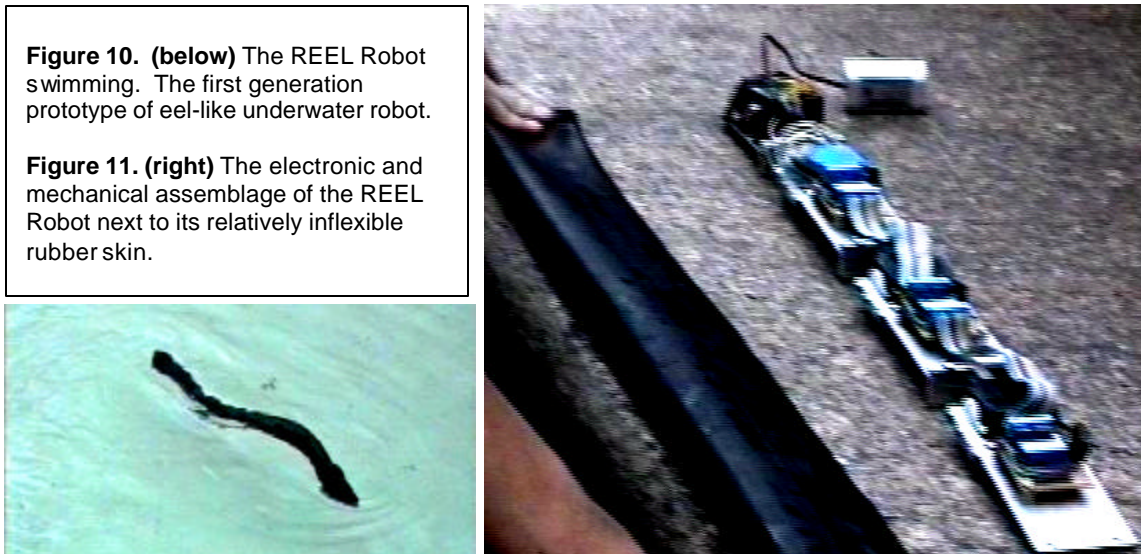
## 2. THE UNDERWATER ROBOT

Previously, Ostrowski and McIsaac developed a geometric framework that encompassed the modeling of anguilliform locomotion and the path planning (and controlling) of a dynamic eel-like system [17]. This framework, once established mathematically, was first substantiated by the use of computer simulations. To

demonstrate the robustness of this mathematical model in the real-life domain, McIsaac and Ostrowski built the REEL robot, a simple RC-controlled four-link robot with actuated servomotor joints. The REEL robot was limited in many ways and I designed and developed a waterproof eel-like robot that extended the usefulness of the robot for testing more complex mathematical models of anguilliform locomotion and increased its robustness, in terms of modularity, efficiency and reproducibility. Modularity is necessary for robustness in a linked robot. Consider when a part or link of the robot is malfunctioning or broken, or even missing. A robust robot will have the ability to continue to function (though less efficiently) despite this impairment and will be simple to fix simply by replacing the module that is broken, missing or malfunctioning. I increased the efficiency of the robot by lowering possible current leakage on the power source to allow more testing time (before the battery needs to be recharged or replaced) and developing an improved mechanical design (so the external forces on the robot more closely model those on an eel). I also closely describe the process of development and implementation to illuminate the simplicity of the design, so McIsaac, Ostrowski and others can easily replicate more models and implement further modifications their research may require.

## 2.1 Mechanical Design

Using the REEL robot as a reference model (see Fig. 10), I first devised the mechanical structure of the robot. I retained the basic design of the first model (see Fig. 11): a series of aluminum plates, comprising the links of the discrete robotic eel, connected by servomotors serving as the actuating joints. In my model, however, the number of links was increased, from four to five, to improve the symmetry of the robot. This change resulted in a few improvements.



Increased symmetry in the robot more closely represents the mathematical model and the robot's accuracy in path following will increase. It also allows the development of new gaits for locomotion not possible in the three-link simulation and four-link robot.

Once the number of links was chosen, we selected the shape of and material for the links. Using design software (ProEngineer v.20), I created 3-dimensional drawings of a cylindrical ellipse with modifications to accommodate the aluminum plates and parts needed to assemble the robot (see Figures 12, 13). Plastic shell structures were produced from these ProE computer designs using a Stratasys FDM (fused deposition modeling) prototyping machine. These shells have three purposes. First, and most important, they better approximate the actual shape of an eel. Having a similar body shape to an eel, in a dynamic aquatic environment, ensures that the model is subjected to similar environmental forces. Since the mathematical model was derived from biological eels and incorporated an approximation of their shape, it will more accurately

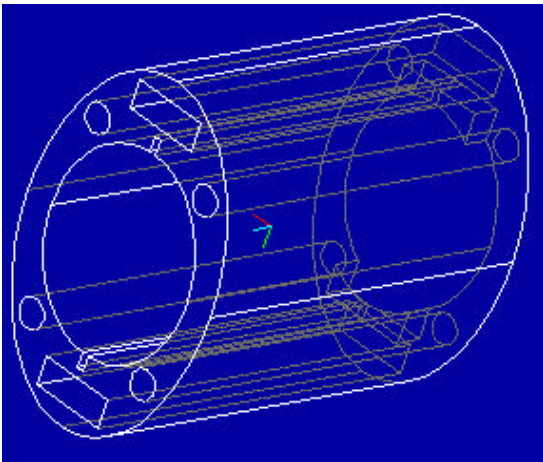


**Figure 12.** Line drawing of elliptical shell link.

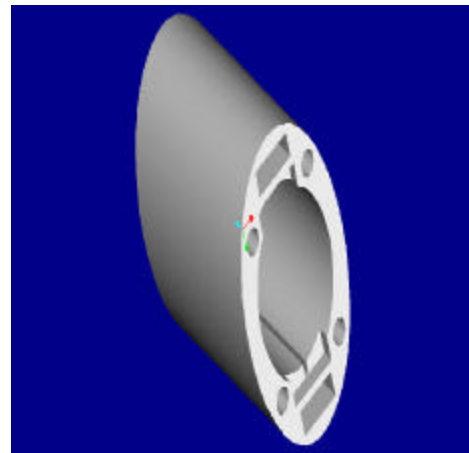


**Figure 13.** Shaded 3D image of link.

**Figure 14.** Line drawing of ellipsoid nosecone.

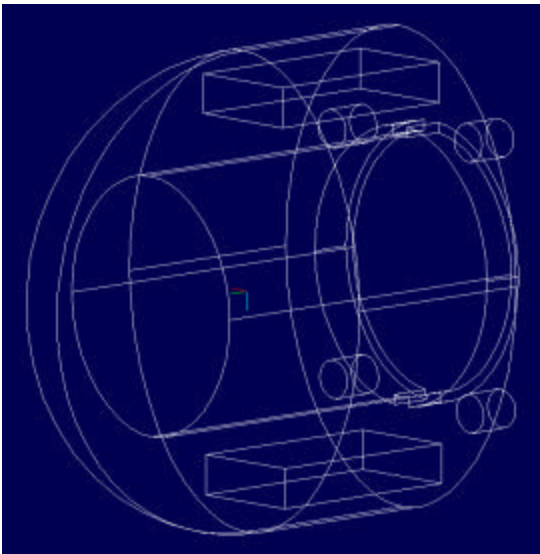
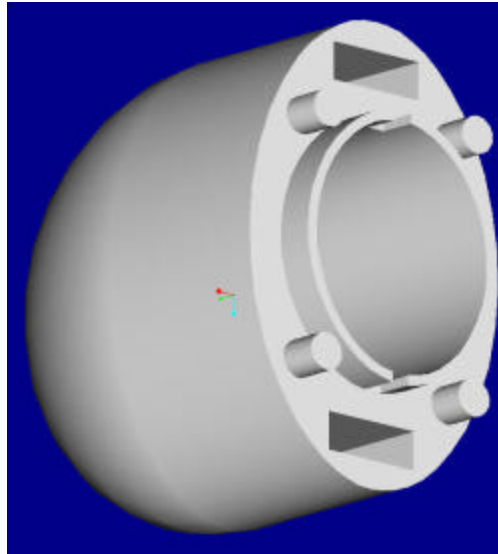


**Figure 15.** Shaded 3D image of nosecone.



describe a robot similarly shaped to the same biological eels. Second, the plastic shells provide a means of buoyancy for the robot in water. The plastic part was designed with air spaces to decrease its density relative to water and to counteract the high density of



the metal and motors, so that the eel has overall neutral buoyancy in water (achieved with the added buoyancy of inflated balloons placed the empty cavities of the shells). Third, the plastic shells house the electronic hardware and “backbone” of aluminum, so that drag is reduced (see Fig. 14). An additional part, necessary to house the battery and to decrease drag in the forward direction, was an ellipsoid nose cone (see Figures 14, 15). I designed this part with ProEngineer software also and then manufactured two plastic parts, one for each end, to retain the symmetry of the robot (see Fig. 17).

The mechanical model still needs further modification to improve its land-traversing capabilities. One alternative we have implemented, is the use of lateral protrusions along the bottom of the plastic shells (on the links, Fig. 18). These modifications roughly mimic the function of the unique belly scales of land-based snakes, to increase lateral resistance while decreasing ventral friction. However, it is important that mass is homogeneously distributed along the length of the body and that the body retains symmetry among its contact points (parts of the body that interact with the environment). Unfortunately, our robot model is not sufficiently homogeneous in mass distribution laterally or longitudinally nor does it have equal contact with the ground on the three middle links of the five-link robot that have the belly-scale modifications. We are presently attempting to improve its performance on land.

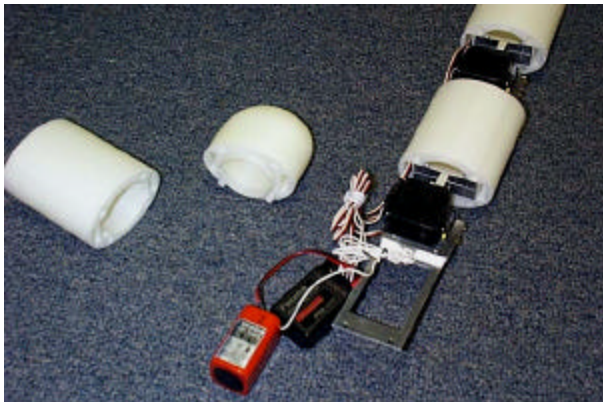


**Figure 16. (right)** Parts of the robot: from left, elliptic cylindrical plastic shell link; ellipsoid nosecone; exposed end of assembled robot showing the NiCd battery, receiver, aluminum plate link, servomotor and the rest of the eel robot.

**Figure 17. (below)** Symmetry of 5-Link Robot, shown fully assembled with nose



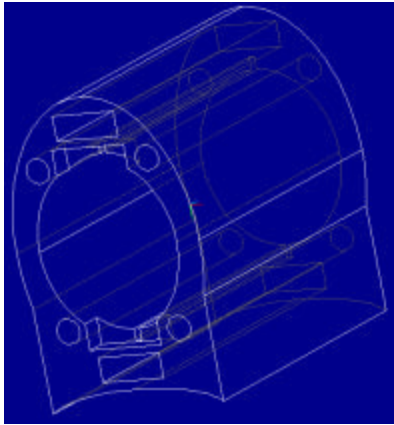
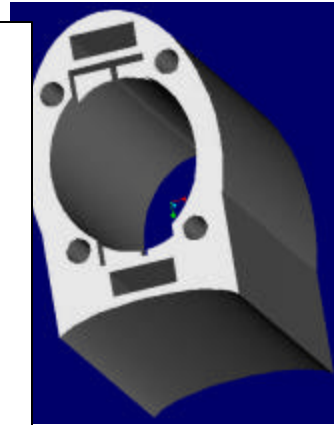


**Figure 18.**

**(left)**  
Line Drawing of Modified Link—Mimics Snake Belly Scales

**(right)**  
Shaded 3D Model of Modified Link—for increased lateral resistance and decreased ventral friction on land.



## 2.2 Electrical Design

The next step, after the mechanical design, was the electrical control design. The previous model had used a Basic Stamp II as an intermediate controller that translated the gait input from the computer to binary inputs that the transmitter then sent as width-modulated pulses to the receiver (and servomotors) in the eel-robot. However, with increased links in my model, the number of joints (and thus servomotors) increased from 3 to 4. Since the set of each angle input for each motor had to reach the receiver (the robot) simultaneously for the correct body motion to occur, the Basic Stamp II was replaced with another intermediate controller that could send the larger set of data simultaneously to the transmitter. I assisted Dan Walker of the GRASP Laboratory in making a PIC micro-controller that fit our specifications (refer to [18] for further explanation). The PIC has four links (can be connected to four separate transmitters) and specifies 2 channels for each link. One channel communicates the joints and the other, the associated positions of the output shaft for each servomotor joint. This robot model requires the use of only one link (see Fig. 17). However, if higher degrees of freedom are desired, the larger number of links could still be controlled with the same electrical hardware and the use of multiple transmitters (one on each link of the PIC micro-controller controlling 4 motors each for a maximum control limit of 16 motors). This electronic hardware design required a high-level computer interface. The software, EelCtrl.exe, provides a Windows interface that gathers input the user types to the computer, computes the necessary joint angles for the motion chosen and sends outputs to the PIC micro-controller as periodic binary signals that encode the set of joints and their associated angles determined for each cycle (of locomotion gait). The algorithm control is discussed in Section 3.3.

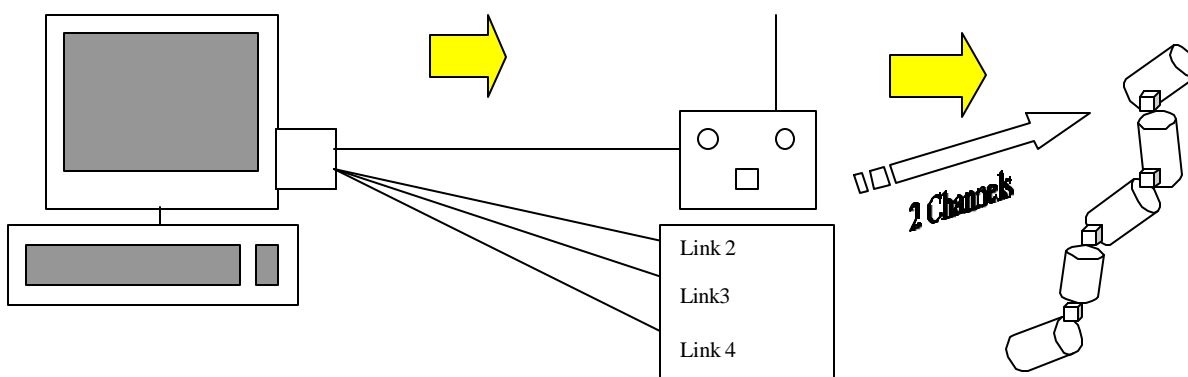


**Figure 19.** Diagram of Control Hardware.

Computer receives input from user and sends a binary signal as output to PIC micro-controller. The PIC converts this to a pulse signal sent on a link to a transmitter. The transmitter sends pulse-width modulated signals to the receiver in the eel-like robot which changes the current and ultimately, the output shaft position) of each motor.

### 2.3 Waterproof Design

In order for this electronic design to function, the electronic hardware must be waterproofed. I researched many alternative methods of waterproofing the robot. I first considered creating a waterproof hull made of more flexible material than in the original prototype (see thick rubber tube covering in Figure 8), such as Gore-Tex™ Ocean Technology waterproof fabrics. There were many complications to this design, however. The seams for a fabric hull would be difficult to seal against water seepage. As a result, the waterproof hull would be difficult to open and close, when it became necessary to replace parts or recharge the battery. So a flooded hull would allow easier maintenance of the robot, but would require each individual electronic component to be waterproofed well to prevent short-circuiting or current leakage (a drain on the energy source). After researching many different compounds with respect to their waterproofing properties, methods of applications, and compatibility with the plastics and hardware of the robot, I decided to coat the electronics with an epoxy resin system. Using epoxy resins, coupled with waterproof AC converters (for recharging the battery), water-resistant servomotors (Futaba S9303 High Torque/Metal Gear/Dust and Water Resistant Servomotors) and dielectric grease (to seal around the output shaft of the motors), I developed a waterproof design that retains the modularity of the mechanical structure. This design has been successfully implemented on the robot and we have shown the waterproof robot to function in an aquatic environment (see Robot Specifications in Section 7.1). The modularity and reproducibility of the robot has also been demonstrated.<sup>1</sup>

<sup>1</sup> After an accident, the plastic housing of the fourth servomotor broke at the point of its attachment to the fifth link of the robot. This servomotor was easily removed and another servomotor, waterproofed with an epoxy resin coating, was put in its place. However, the robot, with only four links, can still perform three of the anguilliform gaits, and thus has functional robustness.

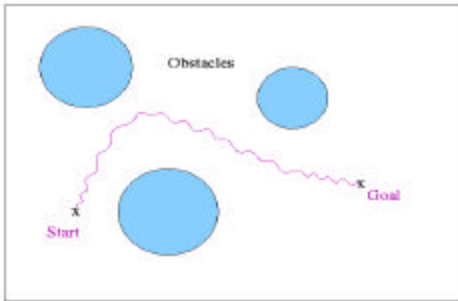
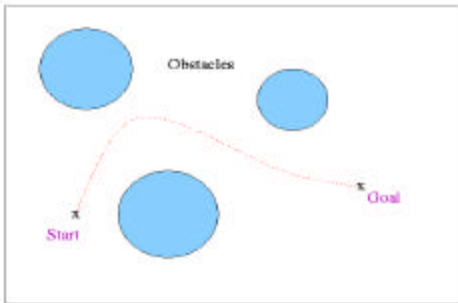
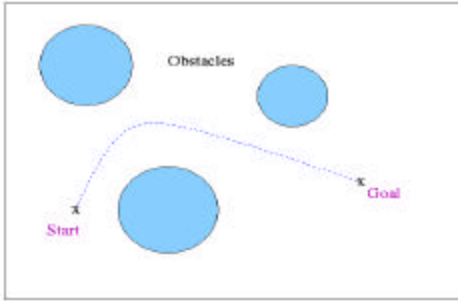
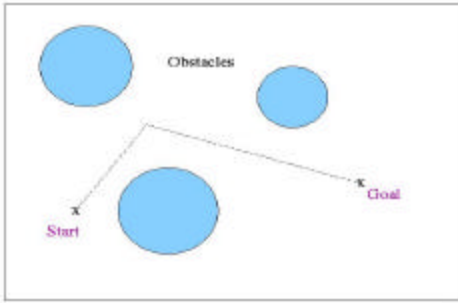
### 3. ANGUILLIFORM LOCOMOTION CONTROL

I have built this waterproof five-link robot to test the framework developed by Ken McIsaac and Jim Ostrowski for steering dynamic robotic locomotion systems [17]. Specifically, my interests are to demonstrate the feasibility of two not yet tested gaits in the real-life domain that were developed from this framework, the sideways motion (crab gait) and change-in-orientation motion (spinning gait), and also to improve the algorithms for the locomotion control of this eel-like underwater robot. I will begin with descriptions of the framework, the novel gaits and the initial algorithms and software developed by McIsaac and Ostrowski that I implemented on the robot and then describe its performance in an aquatic environment and in a terrestrial environment.

#### 3.1 Decomposition of the Motion Planning Problem

One of the most significant aspects of robotics is mobility. Ostrowski and McIsaac have been developing a unifying methodology for studying and controlling locomotion, specifically, a geometric model of dynamic under-actuated locomotion systems. The robustness of this model is that all locomotion systems can ultimately be decomposed into two parts, the position and orientation of the system (the change in position and orientation is the robot's motion) and the shape or internal configuration of the robot (the input is the change in shape). This model seeks to encompass the simple, kinematic locomotion of actuated (direct control of parts that cause motion) robots and the more complex case of under-actuated robotic locomotion systems. This is accomplished by creating a hierarchical geometric structure [17]. At the highest level of abstraction, all locomotion is encoded as a simple, omnidirectional kinematic approximation (where all directions of motion are directly actuated by inputs and can be visualized as a series of connected linear displacements of the body at a constant velocity). The next level considers a kinematic approximation with constrained control inputs (all directions of motion are not directly controlled by the inputs and can be visualized as a continuous curve of body motion with velocity constraints). This level can then be encoded into an equivalent dynamic system with restricted (cyclic) inputs (inputs are functions of shape changes and body momentum and motion can be visualized as sum of body velocity in inertial frame and momentum of body). At the lowest level of the hierarchy, the dynamics are fully described by the coupling between cyclic changes in shape, external forces and constraints (motion can be visualized as the undulatory curve closely mimicking locomotion of eels). This hierarchy is pictorially represented in Figure 18. The equations encoding the information between the hierarchical levels can be applied to most systems, but the equations for the input and momentum must be determined uniquely for each system.





1. Determine goal configuration (perform path planning) assuming an omni-directional (unconstrained) kinematic model

2. Find a kinematic approximation to a class of dynamic systems.

3. Build motion plans for the equivalent kinematic system.

4. Use approximate models of the full dynamic system to develop gaits for motion in (possibly) constrained directions.

5. Use the kinematic and dynamic approximations to develop motion plans for the full dynamic system.

**Figure 20.**

**(left)** Pictorial representations of four levels of abstraction.

**(right)** Decompose motion control algorithm

McIsaac and Ostrowski have uniquely determined the equations for anguilliform motion at each abstraction level. At the lowest level, three equations, the fiber equation, the generalized momentum equation and the base equation, describe the full dynamics of the robot system. The fiber equation governs the motion of the system in the position space based on changes in shape and the momentum in the position directions. The generalized momentum equation describes the dynamics of the system in the position directions via the momentum along each of the kinematically unconstrained fiber directions and including a forcing term that allows modeling of control inputs or external

forces from fluid drag or viscous damping. The base equation describes the evolution of the internal shape of the robot in terms of the internal applied forces.

*Full Dynamics:*

$r$  = shape vector of robot  
 $g$  = position and orientation of robot  
 $u$  = input function  
 $I$  = locked inertia tensor  
 $\tau$  = internal forces  
 $\tau_g$  = constraints and external forces  
 $\xi$  = body velocity  
 $\rho$  = body momentum

*Fiber Equation:*

$$\dot{\xi} = (g^{-1})\dot{g} = -A\dot{r} + (I^{-1})\dot{\rho}$$

*Generalized Momentum Equation:*

$$\dot{\rho} = [(r \cdot)^T] \alpha \dot{r} + (\rho^T) \beta \dot{r} + (\rho^T) \gamma \dot{\rho} + \tau_g$$

*Base Equation:*

$$\mathbf{t}(r)\dot{r} = \tau$$

The equivalent dynamic system for the eel-like robot assumes control of the momentum and restricts the input to cyclic (undulatory) shape functions.

*Equivalent Dynamics:*

*Input Function:*

$$u_p = \dot{\rho}$$

*Motion Equation:*

$$\dot{\xi} = (I^{-1})[u_r]\dot{\rho}$$

This dynamic system is further approximated to a kinematic representation of the system with constrained control inputs (an under-actuated system).

*Constrained Kinematic Approximation:*

*Input Function:*

$$u = \dot{r}$$

*Motion Equation:*

$$\dot{\xi} = (g^{-1})\dot{g} = -A\dot{r}$$

Finally, the abstraction reaches the omnidirectional kinematic approximation which describes all directions of motion as an output directly controlled by the input.

*Omnidirectional (Unconstrained) Kinematic Approximation:*

*Input Function:*

$$u = \dot{x} \text{ where } x = (x, y, \theta)$$

I will not prove these results here as they can be found elsewhere [17]. However, the different cyclic inputs used to generate different motions deserve further explanation (i.e. equations of abstraction between full dynamics and equivalent dynamics and constrained kinematics) because they were important in the development of the eel robot.

### 3.2 Mathematical Models of Gaits

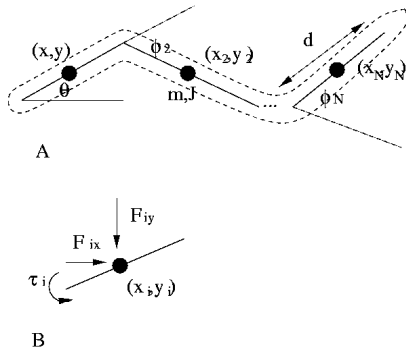


**Figure 21.** Simple representation of eel robot and its links.  
 $g = (x, y, \theta)$  of center link  
 $r =$  vector of all  $\phi(l)$  for each link,  $l$ , except center link  
 $q = (g, r)$

Then:

$$\begin{aligned} \xi &= (g^{-1})g\dot{g} = -A(r)r\dot{r} + (I^{-1})(r)\dot{\rho} \\ \rho\dot{r} &= [(r\dot{r})^T] \sigma_{r\dot{r}} r\dot{r} + (r)\dot{r} + (\rho^T T) \sigma_{\rho\dot{\rho}} (r)\dot{\rho} + \\ &+ (\rho^T T) \sigma_{\rho\dot{\rho}} (r)\dot{\rho} + \tau g \\ \tau_i &= \eta(r)_i r\dot{r} + \alpha(r)_i \dot{\rho} \end{aligned}$$

Using the definitions and equations in Figure 19 to describe the robot eel, the parameters that determine the different gaits can be solved for. Ultimately, understanding these gait parameters will allow us to describe the input function that will result in the desired gait motion. By doing a perturbation analysis, McIsaac has shown the Taylor expansion of the momentum based on the sinusoidally-varying joint angles ( $r$ ) and some scaling parameter. The results from this show the following relationships:

$$\rho\dot{r}(0) = 0 \quad \rho\dot{r}(0) = 0 \quad \rho\dot{r}(i) = \alpha_i(r_0) r\dot{r} + \eta_{ij}(r_0) r\dot{r}$$

This equation will have a zero average solution over one gait cycle because  $r(t)$  is periodic (otherwise would generally have a nonzero closed form solution in terms of exponentials of  $\alpha$ ).

$$\rho\dot{r}(i) = \alpha_i(r_0) r\dot{r} + r_1 \kappa(r_0)_{ijk}$$

$r\dot{r}$

(Note:  $\alpha$  and  $\kappa$  tensors are functions of two dimensionless parameters,

where  $\kappa_{ijk} = (\delta\eta_{jk} / \delta r_i)$

in this

the dominant term

$J = \text{link inertia} / (\text{link mass} \cdot \text{link length})$  and negligible term

equation ignore

$\lambda = \text{approximated coefficient of external friction} / \text{link mass}$

$(\delta\alpha / \delta r)_i r_1$

The form of  $\alpha$  determines whether there exists coupling between the forcing terms in a given direction and momentum generation in unrelated directions. The last equation allows us to design different gaits by analyzing the symmetry of the  $\kappa$  term and its coupling to the gait phasing ( $\phi_i = A \sin(\omega t + i\phi) + \psi$ ).

**Figure 22.** Table of Gaits for 3- and 5-Link Systems and Their Gait Control Parameters

A=gait amplitude,  $\omega$ =gait frequency,  $\psi$  =offset,  $\phi_i$  = gait phasing, see Section 6 Appendix B about fore-aft symmetry

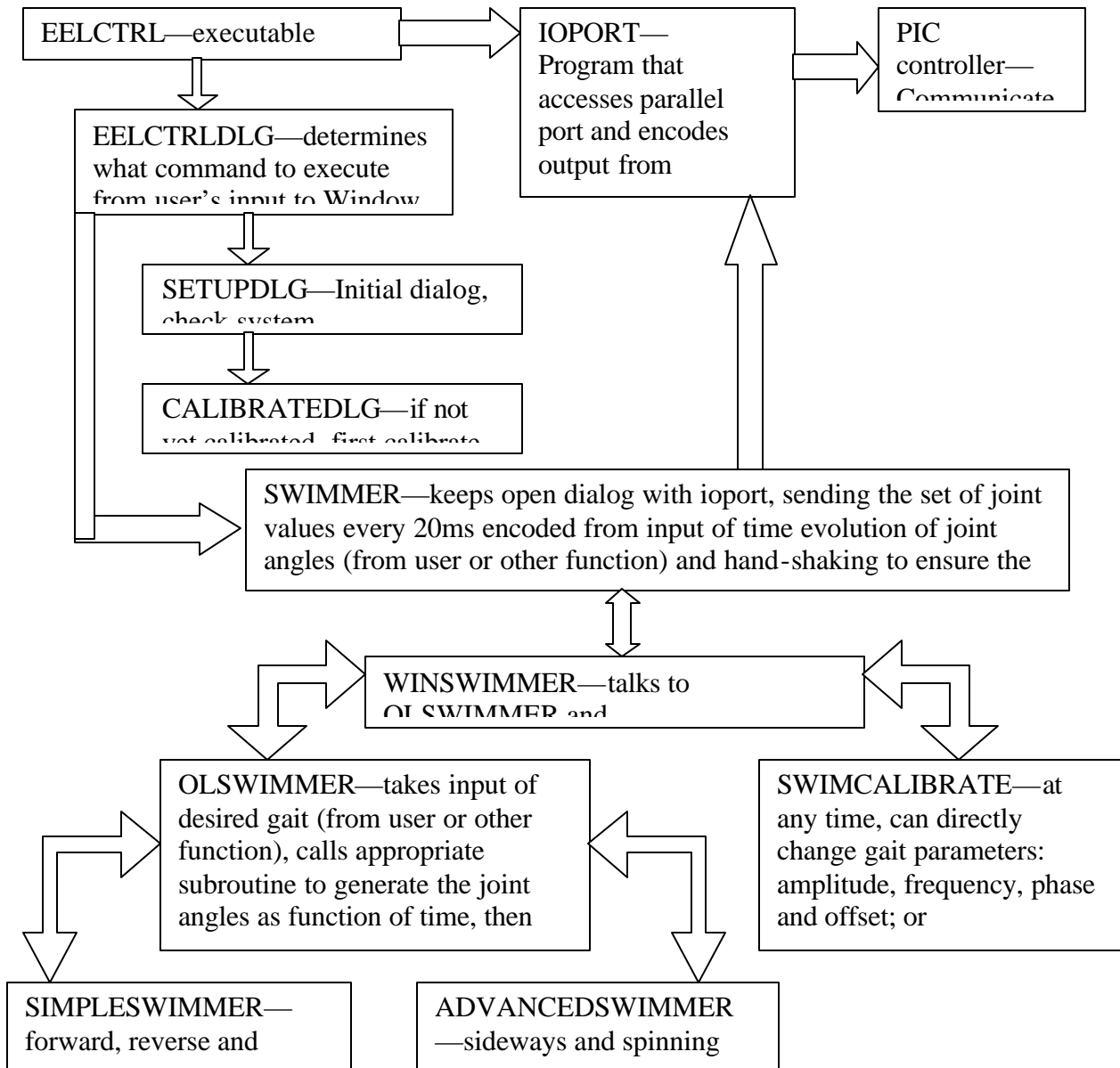
	Three Link Robot Eel (simplest undulatory model)	Five Link Robot Eel (more degrees of freedom)
<b>Forward Gait</b> $\psi = 0$ $k = \text{ave}(r, \kappa_1, r \&)$	$\alpha = \begin{matrix} 0 & 0 & 0, \text{ no coupling} \\ & 0 & \alpha_{22} & 0, \\ & 0 & 0 & \alpha_{33} \end{matrix}$	$\alpha = \begin{matrix} \alpha_{11} & 0 & 0, \text{ no coupling} \\ & 0 & \alpha_{22} & 0, & \psi = 0 \\ & 0 & 0 & \alpha_{33} \end{matrix}$
	$\kappa_1 = \text{fore-aft symmetry}$	$\kappa_1 = \text{fore-aft symmetry}$
	$\kappa_2 = 0$	$\kappa_2 = 0$
	$\kappa_3 = 0$	$\kappa_3 = 0$
	$\rho \& 1 = (A^2)\omega \sum k \sin(-n\phi)$	$\rho \& 1 = (A^2)\omega \sum k \sin(-n\phi)$
<b>Turning Gait</b> $\psi = \text{offset} = r_1 = -r_2$	$\alpha = \begin{matrix} \alpha_{11} & 0 & \alpha_{13}, \text{ coupling between} \\ & 0 & \alpha_{22} & 0, \text{ turning and forward} \\ & \alpha_{31} & 0 & \alpha_{33}, \text{ momentum} \end{matrix}$	$\alpha = \begin{matrix} \alpha_{11} & 0 & \alpha_{13} \\ & 0 & \alpha_{22} & 0 \\ & \alpha_{31} & 0 & \alpha_{33} \end{matrix}$
	$\kappa_1 = \text{fore-aft symmetry}$	$\kappa_1 = \text{fore-aft}$
	$\kappa_2 = (\text{fore-aft symmetry})^{-1}$	$\kappa_2 = (\text{fore-aft})^{-1}$
	$\kappa_3 = \text{fore-aft symmetry}$	$\kappa_3 = \text{fore-aft}$
	$\rho \& 1 = (A^2)\omega \sum k_1 \sin(-n\phi)$ $\rho \& 2 = (A^2)\omega \sum k_2 \sin(-n\phi)$	$\rho \& 1 = (A^2)\omega \sum k \sin(-n\phi)$
<b>Sideways Gait</b> $\psi = r_1 = r_2$	$\alpha = \begin{matrix} \alpha_{11} & \alpha_{12} & 0, \text{ coupling between} \\ & \alpha_{21} & \alpha_{22} & 0, \text{ forward and sideways} \\ & 0 & 0 & \alpha_{33}, \text{ momentum} \end{matrix}$	$\alpha = \begin{matrix} \alpha_{11} & 0 & \alpha_{13}, \text{ no coupling} \\ & 0 & \alpha_{22} & 0 \\ & \alpha_{31} & 0 & \alpha_{33} \end{matrix}$
	$\kappa_1 = \text{fore-aft symmetry}$	$\kappa_1 = \text{fore-aft}, \text{ no forward momentum}$
	$\kappa_2 = \text{fore-aft symmetry}$	$\kappa_2 = (\text{fore-aft})^{-1}$
	$\kappa_3 = (\text{fore-aft symmetry})^{-1}$	$\kappa_3 = \text{fore-aft}, \text{ no angular momentum}$
	$\rho \& = 0$ over one cycle travel in circular path	$\rho \& 1 =$ $\rho \& 2 = (A^2)\omega \sum k_2 \sin(-n\phi)$
<b>Spinning Gait</b>	NOT POSSIBLE	$\alpha = \begin{matrix} \alpha_{11} & 0 & \alpha_{13}, \text{ no coupling} \\ & 0 & \alpha_{22} & 0 \\ & \alpha_{31} & 0 & \alpha_{33} \end{matrix}$
	–	$\kappa_1 = \text{fore-aft}, \text{ no forward motion}$
	–	$\kappa_2 = \text{fore-aft}, \text{ no sideways motion}$
	–	$\kappa_3 = (\text{fore-aft})^{-1}, \text{ only angular momentum}$
$k_3 = r, \kappa, r \&$	–	$\rho \& 3 = (A^2)\omega \sum k_2 \sin(-n\phi)$



This table helps organize the components of the different motions for each gait. The next step is to organize a series of gaits for periods of time in order to follow a desired path and reach some goal state (or destination).

### 3.3 Algorithm for Locomotion Control

Dynamic locomotion control can be decomposed into four steps, momentum generation, steering, momentum degeneration and error corrections. Hybrid system necessary because the system has continuous time dynamics but the controls are generated over discrete intervals (input periods) with discrete mode-switching between gaits. See diagram below for description of algorithm control organization (Figure 23).



## 4. CONCLUSIONS AND RECOMMENDATIONS

This model of the eel-like robot has some successful aspects and a few problems that still need to be solved. One successful aspect is the similarity of application of robot on land or in water. The previous REEL robot was only able to move on land by orienting onto its side and moving in an inchworm-like fashion. Now, the robot can be placed upright (on its belly) and shown to move using the same sinusoidal gaits as in water. The forward motion of the robot, both on land and in water, has an offset of some value that causes the robot to move in a curve rather than a relatively straight path. This same offset seems to affect the other gaits as well (though the eel robot can successfully execute 4 distinct gaits and their reverse motion). Despite my attempts to recalibrate (re-zero the motors to a straight initial configuration), the new calibration values do not seem to be incorporated into the higher-level swim programs. I recommend possible solutions to improve this communication problem in the software design.

The model does, however, have neutral buoyancy and the electrical hardware has been shown to be waterproof. The neutral buoyancy was reached with the aid of inflated balloons in the body cavities and some ballast in the tail (end link not containing the receiver and battery). The process of creating symmetric buoyancy was tedious and imprecise. I also propose other methods of reaching neutral buoyancy in the eel robot that may improve the eel robot's performance.

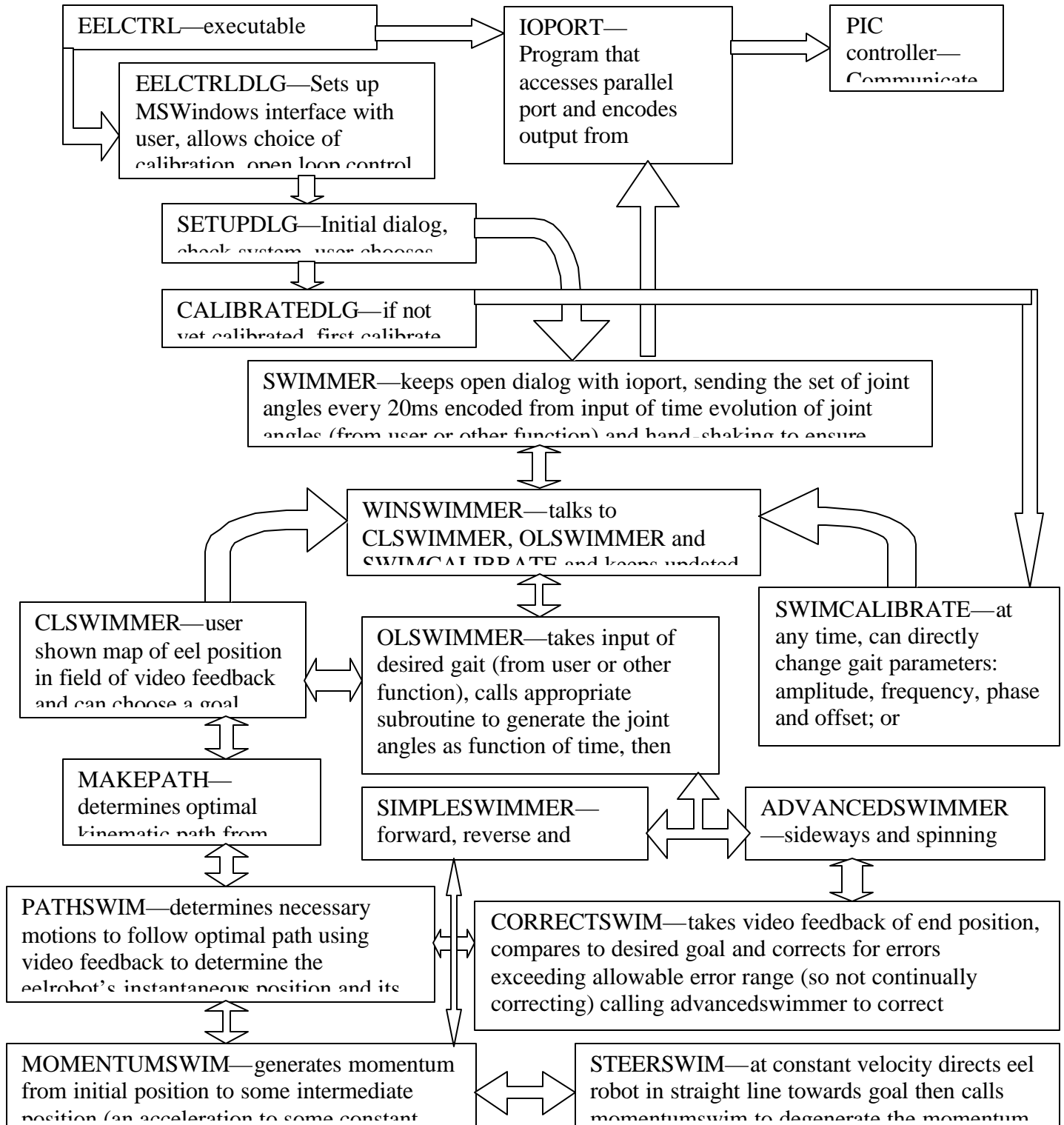
We have shown the successful modularity of the current robot model (described above). The battery (power source) is readily accessible for recharging or replacement.

### 4.1 Suggestions for Improving the Robot's Performance

The performance of the robot would improve with more homogeneous weight distribution along the length of the body. To accomplish this, buoyancy could be added to the nosecone (where the battery now resides) and the battery moved either to the cavity of the second link (more feasible because less wiring) or in the tail-cone (now empty). Also, machining out the center area of the aluminum plates within each link (just as the center of the first link containing the receiver is machined) could easily reduce the total mass of the eel. Perhaps some medium other than inflated balloons could be used for buoyancy, such as styrofoam. Since balloons deflate with time, styrofoam or some similar substance would allow more uniform buoyancy and would be constant over time (it would not require frequent adjustment). Finally, a brightly colored nylon "skin" would increase the efficiency of the eel robot (less vortices and waves would be generated at the joints between links to create greater drag forces) and would increase the visibility of the eel robot (depending on the color of the "skin"). Increased visibility of the eel robot is necessary for further control development that uses visual feedback of robot position for path planning problems (described more below).

### 4.2 Suggestions for Closed-Loop Control Algorithm

I will suggest some algorithm modifications and further designs for implementation with the robot I built. I believe a simpler algorithm will have better communication among the various functions and increase the efficiency of the software design. See diagram below (Figure 24):



## 5. ACKNOWLEDGEMENTS

I owe thanks to Ken McIsaac and Jim Ostrowski for sharing their ideas and results on anguilliform locomotion and their REEL robot. I appreciated the use of their laboratory and supplies. I also would like to thank Aveek Das for taking the time to help me with any problems I encountered in the development of this robot. Other members of the laboratory and SUNFEST program provided valuable encouragement, advice and ideas along the way. This paper was improved significantly with the help of Janice Fisher and Aveek Das.

## 6. REFERENCES

- [1] G.S. Chirikjian and J.W. Burdick. A Modal Approach to the Kinematics of Hyper-Redundant Manipulators. *Robotics and Mechanical Systems Report RMS-89-03, School of Engineering and Applied Science, California Institute of Technology*. Pasadena, CA: September 1989.
- [2] G.S. Chirikjian and J.W. Burdick. The Kinematics of Hyper-Redundant Locomotion. *IEEE Trans. on Robotics and Automation*, 11(6):781-793, 1995.
- [3] University of Pennsylvania, GRASP Laboratory, and Woods Hole Oceanographic Institute, Deep Submergence Laboratory. Subsea Teleprogramming. Information available electronically at <http://www.cis.upenn.edu/~sayers/tele/subsea.html>, 1995.
- [4] L.L. Whitcomb and D.R. Yoerger. A New Distributed Real-Time Control System For The JASON Underwater Robot. In *Proc. IEEE Intl. Workshop on Intelligent Robots and Systems (IROS)*, Yokohama, July 1993.
- [5] Massachusetts Institute of Technology, Ocean Engineering Testing Tank (TowTank), Biomimetics Project. RoboTuna and RoboPike. Information available electronically at <http://web.mit.edu/towtank/www/projects.html>, 1999.
- [6] M.S. Triantafyllou and G.S. Triantafyllou. An Efficient Swimming Machine. *Scientific American*, pp. 64-70, March 1995.
- [7] Northeastern University Marine Science Center. Biomimetic Underwater Robot Program (BURP). Ambulatory Underwater Robot. Information available electronically at <http://www.dac.neu.edu/msc/burp.html>, 1999.
- [8] J. Ayers and J. Crisman. The Lobster as a Model for an Omnidirectional Robotic Ambulation Control Architecture. In R. Beer, R. Ritzman, and T. McKenna, editors, *Biological Neural Networks in Invertebrate Neuroethology and Robots*, pp. 287-316. Academic Press, 1992.
- [9] IS Robotics Research Division. Autonomous Legged Underwater Vehicle. Information available electronically at <http://www.isr.com/research/ariel.html>, 1999.
- [10] C.M. Breder. The Locomotion of Fishes. *Zoologica*, 4:159-297, 1926.
- [11] J. Gray. Studies in Animal Locomotion. I. The Movement of Fish with Special Reference to the Eel. *Journal of Experimental Biology*, 10:88-104, 1933.



- [12] G.B. Gillis. Environmental Effects on Undulatory Locomotion in the American Eel *Anguilla rostrata*: Kinematics in Water and on Land. *Journal of Experimental Biology*, 201:949-961, 1998.
- [13] S. Hirose. *Biologically Inspired Robots: Snake-Like Locomotors and Manipulators*. Translated by Peter Cave and Charles Goulden. Oxford University Press, Oxford, 1993.
- [14] Microsoft Corporation. Microsoft Illustration, "Snake Locomotion," Microsoft(R) Encarta(R) 96 Encyclopedia. Information available electronically at <http://www.kwic.com/~pagodavista/snkmove.htm>, 1993-1995.
- [15] S. Grillner and S. Kashin. On the Generation and Performance of Swimming in Fish. In: R. M. Herman, S. Grillner, P. S. G. Stein, D. G. Stuart (eds). *Neural Control of Locomotion*. Plenum, New York, pages 181-201.
- [16] K.A. McIsaac and J.P. Ostrowski. A Geometric Approach to Anguilliform Locomotion: Simulation and Experiments with an Underwater Eel Robot. In *Proc. IEEE Intl. Conf. Robotics and Automation*, volume 1, pp. 2843-2846, Detroit, MI, 1999.
- [17] K.A. McIsaac and J.P. Ostrowski. A Framework for Steering Dynamic Robotic Locomotion Systems. In *Workshop on Algorithmic Foundations of Motion Control (WAFR)*, 2000.
- [18] D.B. Walker. Remote Manipulation of Mobile Robots Using Stock Radio Components. University of Pennsylvania, GRASP Laboratory, 1999.

## 6. APPENDICES

### 6.1 Appendix A

#### Robot Specifications:

Total Length:	~35.5 inches
Maximum Width:	2 inches
Maximum Height:	~3.7 inches

#### Link Specifications:

Link 1: Nose Cone + Battery + Link + Receiver	
Maximum Height:	3 inches
Link 2-4: Link + Belly Scales	
Maximum Height:	~3.7 inches
Link 5: Link + Tail Cone	
Maximum Height:	3 inches

#### Joint Specifications:

Futaba Servomotors:	S9303 High Torque/Metal Gear/ Dust and Water Resistant
coated in:	epoxy resin, with dielectric grease around the output shaft

Total Mass:

#### Material Sources:

Link plates and arms for joint attachment:	Aluminum
Plastic Shells Manufactured in the Stratasys FDM machine: ( <i>more information available electronically at:</i> <a href="http://www.stratasys.com">www.stratasys.com</a> )	P400 (a polystyrene)
West System Epoxy Resin: ( <i>more information available electronically at:</i> <a href="http://www.concentric.net/~westsys">www.concentric.net/~westsys</a> )	Epoxy Resin 105 Hardener 205 Microfibers 403 Aluminum-based Barrier Coat Additive
Dielectric Grease:	Dynatex Part No. 49635
Waterproof AC Converters	

## 6.2 Appendix B

**Fore-Aft Symmetry** implies that  $\hat{e}$  is a square matrix of the form  $\begin{bmatrix} x & y \\ -y & -x \end{bmatrix}$ . This implies that both ends of the eel are moving in the same positive direction to achieve some translation.

**Inverse fore-aft symmetry** implies  $\hat{e}$  is a square matrix of the form  $\begin{bmatrix} x & y \\ y & x \end{bmatrix}$  which means that the ends are moving in opposite directions and canceling each other, resulting in angular motion.

DESIGNING AN UNDERWATER EEL-LIKE ROBOT AND DEVELOPING ANGUILLIFORM LOCOMOTION CONTROL .....	119
Tamara Knutsen, Harvard University	
ABSTRACT.....	119
1. MOTIVATION .....	119
1.1 Underwater Robotic Systems.....	120
1.2 Biomimetic Robotic Technology.....	120
1.3 Biological Models of Locomotion.....	122
1.4 Mathematical Models of Locomotion.....	123
2. THE UNDERWATER ROBOT .....	124
2.1 Mechanical Design.....	125
2.2 Electrical Design.....	128
2.3 Waterproof Design.....	129
3. ANGUILLIFORM LOCOMOTION CONTROL .....	130
3.1 Decomposition of the Motion Planning Problem.....	130
3.2 Mathematical Models of Gaits.....	133
3.3 Algorithm for Locomotion Control .....	135
4. CONCLUSIONS AND RECOMMENDATIONS .....	136
4.1 Suggestions for Improving the Robot's Performance.....	136
4.2 Suggestions for Closed-Loop Control Algorithm.....	136
5. ACKNOWLEDGEMENTS .....	138
6. REFERENCES .....	138
6. APPENDICES .....	140
6.1 Appendix A.....	140
6.2 Appendix B.....	141